

*Carnegie Observatories Astrophysics Series, Vol. 1:  
Coevolution of Black Holes and Galaxies  
ed. L. C. Ho (Cambridge: Cambridge Univ. Press)*

---

# Formation of Supermassive Black Holes: Simulations in General Relativity

S. L. SHAPIRO  
*The University of Illinois at Urbana–Champaign*

---

## Abstract

There is compelling evidence that supermassive black holes exist. Yet the origin of these objects, or their seeds, is still unknown. We discuss several plausible scenarios for forming the seeds of supermassive black holes. These include the catastrophic collapse of supermassive stars, the collapse of relativistic clusters of collisionless particles or stars, the gravothermal evolution of dense clusters of ordinary stars or stellar-mass compact objects, and the gravothermal evolution of self-interacting dark matter halos. Einstein's equations of general relativity are required to describe key facets of these scenarios, and large-scale numerical simulations are performed to solve them.

## 1.1 Introduction

There is substantial evidence that supermassive black holes (SMBHs) of mass  $\sim 10^6 - 10^{10} M_{\odot}$  exist and are the engines that power active galactic nuclei (AGNs) and quasars (Rees 1998, 2001; Macchetto 1999). There is also ample evidence that SMBHs reside at the centers of many, and perhaps most, galaxies (Richstone et al. 1998; Ho 1999), including the Milky Way (Genzel et al. 1997; Ghez et al. 2000; Schödel et al. 2002).

Since quasars have been discovered out to redshift  $z \gtrsim 6$  (Fan et al. 2000, 2001), the first SMBHs must have formed by  $z_{\text{BH}} \gtrsim 6$ , or within  $t_{\text{BH}} \lesssim 10^9$  yrs after the Big Bang. However, the cosmological origin of SMBHs is not known. This issue remains one of the crucial, unresolved components of structure formation in the early universe. Gravitationally, black holes are strong-field objects whose properties are governed by Einstein's theory of relativistic gravitation — general relativity. General relativistic simulations of gravitational collapse to black holes therefore may help reveal how, when and where SMBHs, or their seeds, form in the universe. Simulating plausible paths by which the first seed black holes may have arisen is the underlying motivation of our investigation (see Fig. 1.1).

## 1.2 The Boltzmann Equation

Various routes have been proposed over the years by which SMBHs or their seeds might arise by conventional physical processes (see, e.g., Fig. 1 in Rees 1984). Some routes are hydrodynamical in nature, such as the formation and collapse of supermassive stars (SMSs), while others are stellar dynamical, like the evolution and collapse of colli-

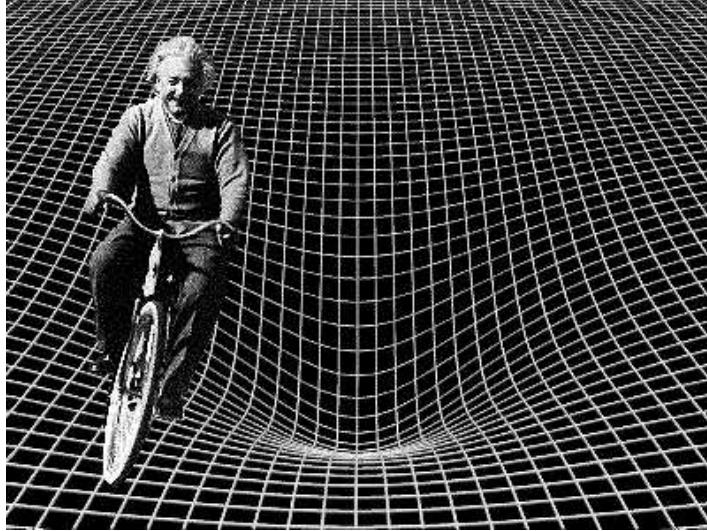


Fig. 1.1. The formation of a black hole is a strong-field gravitational phenomenon in curved spacetime that requires Einstein's equations of general relativity for a description and, in nontrivial cases, numerical simulations for a solution.

sionless clusters. The Boltzmann equation provides a common mathematical framework for comparing competing scenarios:

$$\frac{Df}{Dt} = \left( \frac{\partial f}{\partial t} \right)_{\text{collisions}} . \quad (1.1)$$

In equation (1.1)  $f$  is the phase-space distribution function for the matter, which might be in the form of a gaseous fluid, collisionless particles, and/or stars. The left-hand side of the equation represents the total time derivative of  $f$  following a matter element along its trajectory in phase space. The right-hand side describes the role of collisions in modifying the phase-space distribution along the trajectory. To treat different scenarios the Boltzmann equation must be solved in different physical regimes, all of which share gravitation as the dominant long-range interaction.

Table 1.1 summarizes some of the SMBH formation simulations that we have performed in recent years. Typically, every scenario falls into one of three distinct regimes. In the Vlasov (collisionless Boltzmann) regime the dynamical timescale of the system,  $t_d$ , which is the time for matter to cross from one side of the system to the other, as well as the time to achieve virial equilibrium by violent relaxation, is much shorter than the relaxation timescale  $t_r$ , the time for the system to reach thermal equilibrium via collisions. In pure Vlasov simulations the integration time  $t$  may exceed  $t_d$  but always remains much shorter than  $t_r$ . In such cases collisions can be ignored. The system can be evolved to dynamical (virial) equilibrium, but not thermal equilibrium. In the secularly collisional regime,  $t_d$  again is much shorter than  $t_r$  but the integration time is now much longer than  $t_r$ . Here collisions are crucial in driving the quasi-stationary evolution of the virialized system. Since the timescale for collisions remains much longer than the dynamical timescale, collisions can often be handled perturbatively by tracking the secular drift of the system from one, nearly collisionless,

*S. L. Shapiro*

virialized state to the next. This is the approach adopted in the Fokker-Planck approximation to the Boltzmann equation. In the collision-dominated regime,  $t_r$  is much shorter than  $t_d$  and the system behaves as a fluid. This regime embraces all of hydrodynamics.

Table 1.1 Boltzmann simulations of SMBH formation scenarios

REGIME	Vlasov (Collisionless)	Fokker-Planck (Secularly Collisional)	Fluid (Collision Dominated)
TIME SCALE ORDERING	$t_r \gg t \gg t_d$	$t \gg t_r \gg t_d$	$t \gg t_d \gg t_r$
SCENARIOS	dynamical collapse of a relativistic cluster of (1) compact stars (NSs or stellar-mass BHs) or (2) collisionless particles	“gravothermal catastrophe” drives core contraction of (1) a dense cluster of compact stars; or (2) a dense cluster of ordinary stars; or (3) an SIDM halo	hydrodynamical collapse of an SMS
GRAVITATION	GR	Newtonian	GR, PN*
SPATIAL SYMMETRY	Spherical; Axisymmetrical	Spherical	Spherical; Axisymmetrical; Arbitrary*
COMPUTATIONAL DIMENSIONS	1 + 1; 2 + 1	1 + 1	1 + 1; 2 + 1; 3 + 1*
COMPUTATIONAL TECHNIQUE	particle simulation (matter) + finite-differencing (field)	finite-differencing	finite-differencing

Scenarios considered to date for forming SMBHs, or their seeds, in the Vlasov regime focus on the dynamical collapse of a radially unstable, relativistic cluster of compact stars (neutrons stars or stellar-mass black holes) or collisionless particles. Scenarios in the secularly collisional regime typically involve the gravothermal contraction of a dense cluster of ordinary stars or compact stars which undergo collisions and mergers, leading to a build-up of massive black holes. The gravothermal contraction of a self-interacting dark matter halo (SIDM) in the early universe may also produce a SMBH. Hydrodynamical scenarios typically focus on the collapse of a SMS or gas cloud. Not surprisingly, simulations performed in the different regimes require very different computational approaches. Table 1 indicates that the different scenarios have been tackled by adopting various degrees of spatial symmetry to simplify the calculations. A summary of the results of these simulations is given in the sections below.

### 1.3 Numerical Relativity

Numerical relativity — the art and science of developing computer algorithms to solve Einstein’s field equations of general relativity — is the principal tool needed to sim-

*S. L. Shapiro*

ulate plausible black hole formation processes. The underlying equations are multidimensional, highly nonlinear, coupled partial differential equations in space and time. They have in common with other areas of computational physics, like fluid dynamics and MHD, all of the usual problems associated with solving such nontrivial equations. However, solving Einstein's equations poses some additional complications that are unique to general relativity. The first complication concerns the choice of coordinates. In general relativity, coordinates are merely labels that distinguish points in spacetime; by themselves coordinate intervals have no physical significance. To use coordinate intervals to determine physically measurable (proper) distances and times requires the spacetime metric, but the metric is determined only after Einstein's equations have been solved. Moreover, as the integrations proceed, it often turns out that the original (arbitrary) choice of coordinates turns out to be bad, because, for example, singularities eventually are encountered in the equations. The gauge freedom inherent in general relativity — the ability to choose coordinates in an arbitrary way — is not always easy to exploit successfully in a numerical routine.

The appearance of black holes always poses a complication in a numerical relativity simulation. Black holes inevitably contain spacetime singularities — regions where the gravitational tidal field, the matter density, and the spacetime curvature all become infinite. Encountering such singularities results in some of the terms in Einstein's equations becoming infinite, causing overflows in the computer output and premature termination of the numerical integration. Thus, when dealing with black holes, it is crucial to choose a technique which avoids the spacetime singularities inside. Some of the techniques involve choosing appropriate coordinate gauges that avoid or postpone the appearance of singularities inside black holes. Others involve excising the black hole interiors altogether from the numerical grid.

One of the main goals of a numerical relativity simulation is to determine the gravitational radiation generated from a dynamical scenario. However, the gravitational wave components usually constitute small fractions of the background spacetime metric. Moreover, to extract the waves from the background requires that one probe the spacetime in the far-field or radiation zone, which is typically at large distance from the strong-field central source. Yet it is the strong-field, near-zone region that usually consumes most the computational resources (e.g., spatial grid) to guarantee accuracy. Furthermore, waiting for the wave to propagate to the far-field region usually takes nonnegligible integration time. Overcoming these difficulties to reliably measure the wave content thus requires that a code successfully cope with the problem of dynamic range inherent in such a simulation.

For a recent review of the status of numerical relativity, and a summary of the key equations, see Baumgarte & Shapiro (2003) and references therein.

#### **1.4 Collapse of a Rotating SMS to a SMBH**

SMBHs must be present by  $z_{\text{BH}} \gtrsim 6$  to power quasars. It has been suggested (Gnedin 2001) that even if they grew by accretion from smaller seeds, SMBH seeds  $\gtrsim 10^5 M_{\odot}$  must have formed at  $z \approx 9$  to have had sufficient time to build up to a typical mass of  $\sim 10^9 M_{\odot}$ . A likely progenitor is a very massive object (e.g., an SMS) supported by radiation pressure.

SMSs ( $10^3 \lesssim M/M_{\odot} \lesssim 10^{13}$ ) may form when contracting or colliding primordial gas builds up sufficient radiation pressure to inhibit fragmentation and prevent star formation (see, e.g., Bromm & Loeb 2003). SMSs supported by radiation pressure will evolve in a

*S. L. Shapiro*

quasi-stationary manner to the point of onset of dynamical collapse due to general relativity (Chandrasekhar 1964a,b; Feynmann, unpublished, as quoted in Fowler 1964). Unstable SMSs with  $M \gtrsim 10^5 M_\odot$  and metallicity  $Z \lesssim 0.005$  do not disrupt due to thermonuclear explosions during collapse (Fuller, Woosley, & Weaver 1986). In fact, recent Newtonian simulations suggest that evolved zero-metallicity (Pop III) stars  $\gtrsim 300 M_\odot$  do not disrupt but collapse with negligible mass loss (Fryer, Woosley, & Heger 2001). This finding could be important since the first generation of stars may form in the range  $10^2 - 10^3 M_\odot$  (Bromm, Coppi, & Larson 1999; Abel, Bryan, & Norman 2000). A combination of turbulent viscosity and magnetic fields likely will keep a spinning SMS in uniform rotation (Bisnovatyi-Kogan, Zel'dovich, & Novikov 1967; Wagoner 1969; Zel'dovich & Novikov 1971; Shapiro 2000; but see New & Shapiro 2001 for an alternative). As they cool and contract, uniformly rotating SMSs reach the maximally rotating *mass-shedding limit* and subsequently evolve in a quasi-stationary manner along a mass-shedding sequence until reaching the instability point. At mass-shedding, the matter at the equator moves in a circular geodesic with a velocity equal to the local Kepler velocity (Baumgarte & Shapiro 1999).

It is straightforward to understand the radial instability induced by general relativity in a SMS by using an energy variational principle (Zel'dovich & Novikov 1971; Shapiro & Teukolsky 1983). Let  $E = E(\rho_c)$  be the total energy of a momentarily static, spherical fluid configuration characterized by central mass density  $\rho_c$ . The condition that  $E(\rho_c)$  be an extremum for variations that keep the total rest mass and specific entropy distribution fixed is equivalent to the condition of hydrostatic equilibrium and establishes the relation between the equilibrium mass and central density:

$$\frac{\partial E}{\partial \rho_c} = 0 \implies M_{\text{eq}} = M_{\text{eq}}(\rho_c) \quad (\text{equilibrium}). \quad (1.2)$$

The condition that the second variation of  $E(\rho_c)$  be zero is the criterion for the onset of dynamical instability. This criterion shows that the turning point on a curve of equilibrium mass vs. central density marks the transition from stability to instability:

$$\frac{\partial^2 E}{\partial \rho_c^2} = 0 \iff \frac{\partial M_{\text{eq}}}{\partial \rho_c} = 0 \quad (\text{onset of instability}). \quad (1.3)$$

Consider the simplest case of a spherical Newtonian SMS supported solely by radiation pressure and endowed with zero rotation. This is an  $n = 3$ , ( $\Gamma = 1 + 1/n = 4/3$ ) polytrope, with pressure

$$P = P_{\text{rad}} = \frac{1}{3} a T^4 = K \rho^{\frac{4}{3}}, \quad (1.4)$$

where  $K = K(s_{\text{rad}})$  is a constant determined by the value of the (constant) specific entropy  $s_{\text{rad}} = \frac{4}{3} a T^3 / n$  in the star. Here  $T$  is the temperature,  $n$  is the baryon number density, and  $a$  is the radiation constant. Consider a sequence of configurations with the same specific entropy but different values of central density. The total energy of each configuration is

$$E(\rho_c) = U_{\text{rad}} + W, \quad (1.5)$$

where  $U_{\text{rad}}$  is the total internal radiation energy and  $W$  is the gravitational potential energy. Applying the equilibrium condition (1.2) to this functional yields  $M_{\text{eq}} = M_{\text{eq}}(s_{\text{rad}})$ , i.e. the equilibrium mass depends only on the specific entropy and is independent of central density

*S. L. Shapiro*

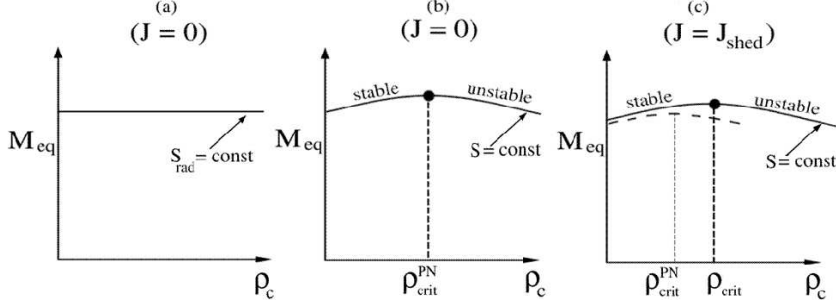


Fig. 1.2. A sketch of mass versus central density along an equilibrium sequence of SMSs of fixed entropy. Panel (a) shows nonrotating, spherical Newtonian models supported by pure radiation pressure; (b) shows nonrotating, spherical PN models supported by radiation pressure plus thermal gas pressure; (c) shows rotating PPN models spinning at the mass-shedding limit.

(see Fig. 1.2a). Applying the stability condition (1.3) then shows that all equilibrium models along this sequence are marginally stable to collapse.

Now let us account for the effects of general relativity. If we include the small (destabilizing) Post-Newtonian (PN) correction to the gravitational field, we must also include a comparable (stabilizing) correction to the equation of state arising from thermal gas pressure:

$$P = P_{\text{rad}} + P_{\text{gas}} = \frac{1}{3}aT^4 + 2nkT, \quad (1.6)$$

where we have taken the gas to be pure ionized hydrogen. Note that  $P_{\text{gas}}/P_{\text{rad}} = 8/(s_{\text{rad}}/k) \ll 1$ . The energy functional of a star now becomes

$$E(\rho_c) = U_{\text{rad}} + W + \Delta U_{\text{gas}} + \Delta W_{\text{PN}}, \quad (1.7)$$

where  $\Delta U_{\text{gas}}$  is the internal energy perturbation due to thermal gas energy and  $\Delta W_{\text{PN}}$  is the PN perturbation to the gravitational potential energy. Applying the equilibrium condition (1.2) now yields  $M_{\text{eq}} \approx M_{\text{eq}}^{\text{Newt}}$  times a slowly varying function of  $\rho_c$  (see Fig. 1.2b). The turning point on the equilibrium curve marks the onset of radial instability; the marginally stable critical configuration is characterized by

$$\begin{aligned} \rho_{c,\text{crit}} &= 2 \times 10^{-3} M_6^{-7/2} \text{ gm cm}^{-3}, \\ T_{c,\text{crit}} &= (3 \times 10^7) M_6^{-1} \text{ K}, \\ (R/M)_{\text{crit}} &= 1.6 \times 10^3 M_6^{1/2}, \end{aligned} \quad (1.8)$$

where  $M_6$  denotes the mass in units of  $10^6 M_{\odot}$ . (Here and throughout we adopt gravitational units and set  $G = 1 = c$ .)

Finally, let us consider a uniformly rotating SMS spinning at the mass-shedding limit (Baumgarte & Shapiro 1999). A centrally condensed object like an  $n = 3$  polytrope can only support a small amount of rotation before matter flies off at the equator. At the mass-shedding limit, the ratio of rotational kinetic to gravitational potential energy is only  $T/|W| = 0.899 \times 10^{-2} \ll 1$ . Most of the mass resides in a nearly spherical interior core, while the low-mass (Roche) envelope bulges out in the equator:  $R_{\text{eq}}/R_{\text{pole}} = 3/2$ . When we include the

*S. L. Shapiro*

contribution of rotational kinetic energy to the energy functional, we must now also include the effects of relativistic gravity to Post-Post-Newtonian (i.e. PPN) order, since both  $T$  and  $\Delta W_{\text{PN}}$  scale with  $\rho_c$  to the same power. The energy functional becomes

$$E(\rho_c) = U_{\text{rad}} + W + \Delta U_{\text{gas}} + \Delta W_{\text{PN}} + \Delta W_{\text{PPN}} + T \quad (1.9)$$

Applying the equilibrium condition (1.2), holding  $M$ , angular momentum  $J$  and  $s$  fixed, now yields  $M_{\text{eq}} \approx M_{\text{eq}}^{\text{Newt}}$  times a slowly varying function of  $\rho_c$  (see Fig. 1.2c). If we restrict our attention to rapidly rotating stars with  $M > 10^5 M_{\odot}$  the influence of thermal gas pressure is unimportant in determining the critical point of instability. The turning point on the equilibrium curve then shifts to higher density and compaction than the critical values for nonrotating stars, reflecting the stabilizing role of rotation:

$$\begin{aligned} \rho_{c,\text{crit}} &= 0.9 \times 10^{-1} M_6^{-2} \text{ gm cm}^{-3}, \\ T_{c,\text{crit}} &= (9 \times 10^7) M_6^{-1/2} \text{ K}, \\ (R_{\text{pole}}/M)_{\text{crit}} &= 427, \\ (J/M^2)_{\text{crit}} &= 0.97. \end{aligned} \quad (1.10)$$

The actual values quoted above for the critical configuration were determined by a careful numerical integration of the general relativistic equilibrium equations for rotating stars (Baumgarte & Shapiro 1999); they are in close agreement with those determined analytically by the variational treatment. The numbers found for the nondimensional critical compaction and angular momentum are quite interesting. First, they are universal ratios that are independent of the mass of the SMS. This means that a single relativistic simulation will suffice to track the collapse of a marginally unstable, maximally rotating SMS of arbitrary mass. Second, the large value of the critical radius shows that a marginally unstable configuration is nearly Newtonian at the onset of collapse. Third, the fact that the angular momentum parameter of the critical configuration  $J/M^2$  is below unity suggests that, in principle, the entire mass and angular momentum of the configuration could collapse to a rotating black hole without violating the Kerr limit for black hole spin (but see below!).

There are several plausible outcomes that one might envision *a priori* for the dynamical collapse of a uniformly rotating SMS once it reaches the marginally unstable critical point identified above. It could collapse to a clumpy, nearly axisymmetric disk, similar to the one arising in the Newtonian SPH simulation of Loeb & Rasio (1994) for the isothermal ( $\Gamma = 1$ ) implosion of an initially homogeneous, uniformly rotating, low-entropy cloud. Alternatively, the disk might develop a large-scale, nonaxisymmetric bar. After all, the onset of a dynamically unstable bar mode in a spinning equilibrium star occurs when the ratio  $T/|W| \approx 0.27$  (see, e.g., Chandrasekhar 1969 and Lai, Rasio, & Shapiro 1993 for Newtonian treatments and Saijo et al. 2001 and Shibata, Baumgarte, & Shapiro 2000a for simulations in general relativity). Since  $T/|W|$  is  $0.899 \times 10^{-2}$  at the onset of collapse and scales roughly as  $R^{-1}$  during collapse due to conservation of mass and angular momentum, this ratio climbs above the dynamical bar instability threshold when the SMS collapses to  $R/M \approx 20$ , well before the horizon is reached. The growth of a bar might begin at this point. Indeed, a weak bar forms in simulations of rotating supernova core collapse (Rampp, Müller, & Ruffert 1998; Brown 2001), but here the equation of state stiffens ( $\Gamma > 4/3$ ) at the end of the collapse, triggering a bounce and thereby allowing more time for the bar to develop. A rapidly rotating unstable SMS might not form a disk at all, but instead collapse entirely to a Kerr

*S. L. Shapiro*

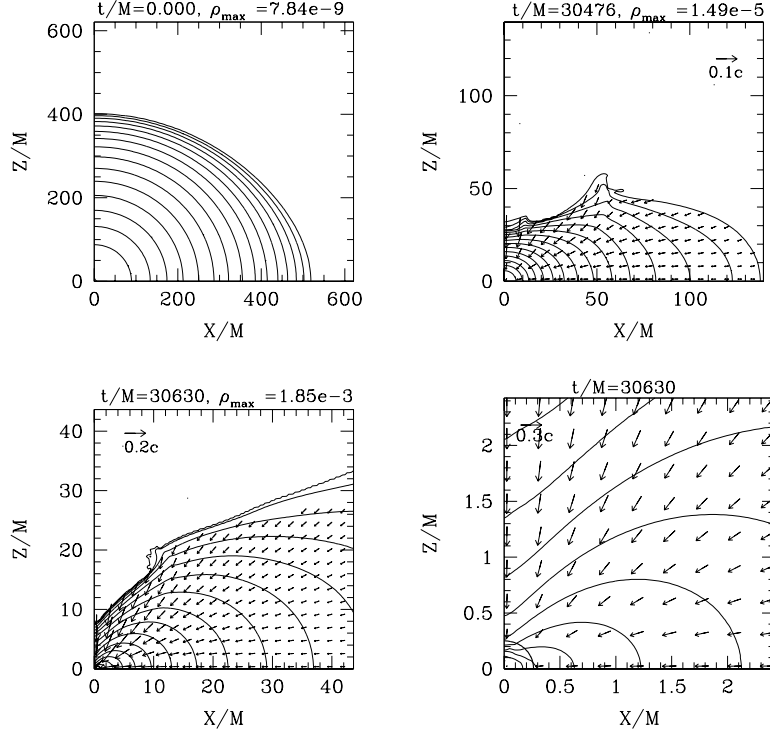


Fig. 1.3. Snapshots of density and velocity profiles during the implosion of a marginally unstable SMS of arbitrary mass  $M$  rotating uniformly at break-up speed at  $t = 0$ . The contours are drawn for  $\rho/\rho_{\max} = 10^{-0.4j}$  ( $j = 0 - 15$ ), where  $\rho_{\max}$  denotes the maximum density at each time. The fourth figure is the magnification of the third one in the central region: the thick solid curve at  $r \approx 0.3M$  denotes the location of the apparent horizon of the emerging SMBH. (From Shibata & Shapiro 2002.)

black hole; not surprisingly, a nonrotating spherical SMS has been shown to collapse to a Schwarzschild black hole (Shapiro & Teukolsky 1979). Alternatively, the unstable rotating SMS might collapse to a rotating black hole *and* an ambient disk.

Two recent simulations have resolved the fate of a marginally unstable, maximally rotating SMS of arbitrary mass  $M$ . Saijo et al. (2002) followed the collapse in full 3D, assuming PN theory. They tracked the implosion up to the point at which the central spacetime metric begins to deviate appreciably from flat space at the stellar center. They found that the massive core collapses homologously during the Newtonian epoch of collapse, and that axisymmetry is preserved up to the termination of the integrations. This calculation motivated Shibata & Shapiro (2002) to follow the collapse in full general relativity by assuming axisymmetry from the beginning (see Fig. 1.3). They found that the final object is a Kerr-like black hole surrounded by a disk of orbiting gaseous debris. The final black hole mass and spin were determined to be  $M_h/M \approx 0.9$  and  $J_h/M_h^2 \approx 0.75$ . The remaining mass goes into the disk of mass  $M_{\text{disk}}/M \approx 0.1$ . A disk forms even though the total spin of the progenitor



*S. L. Shapiro*

star is safely below the Kerr limit. This outcome results from the fact that the dense inner core collapses homologously to form a central black hole, while the diffuse outer envelope avoids capture because of its high angular momentum. Specifically, in the outermost shells, the angular momentum per unit mass  $j$ , which is strictly conserved on cylinders, exceeds  $j_{\text{ISCO}}$ , the specific angular momentum at the innermost stable circular orbit about the final hole. This fact suggests how the final black hole and disk parameters can be calculated *analytically* from the initial SMS density and angular momentum distribution (Shapiro & Shibata 2002). The result applies to the collapse of *any* marginally unstable  $n = 3$  polytrope at mass-shedding. Maximally rotating stars which are characterized by stiffer equations of state and smaller  $n$  (higher  $\Gamma$ ) do not form disks, typically, since they are more compact and less centrally condensed at the onset of collapse (Shibata, Baumgarte, & Shapiro 2000b).

The above calculations show that a SMBH formed from the collapse of a maximally rotating SMS is always born with a “ready-made” accretion disk. This disk might provide a convenient source of fuel to power the central engine. The calculations also show that the SMBH will be born rapidly rotating. This fact is intriguing in light of suggestions that observed SMBHs rotate rapidly (e.g., Wilms et al. 2001; Elvis, Risaliti, & Zamorani 2002).

## 1.5 Collapse of Collisionless Matter to a SMBH

Zel’dovich & Podurets (1965) speculated that sufficiently compact, relativistic clusters of collisionless particles (e.g., relativistic star clusters) would be unstable to gravitational collapse. It has taken considerable theoretical effort to prove that this speculation is correct. For a given distribution function  $f = f(E)$ , one can construct a sequence of spherical equilibrium clusters parametrized by the gravitational redshift at the cluster center,  $z_c$ . One can then plot a curve of fractional binding energy  $E_b/M_0 = 1 - M/M_0$  vs.  $z_c$  along the sequence. Linear perturbation theory, implemented via a variational principle and trial functions, shows that the onset of radial instability occurs near the first turning point on such a binding energy curve (Ipser & Thorne 1968; Ipser 1969; Fackerell 1970). A rigorous theorem has been proven that spherical equilibrium configurations are stable, at least up to the first turning point on the binding energy curve (Ipser 1980). Numerical simulations have shown that all spherical configurations beyond the first turning point are dynamically unstable (Shapiro & Teukolsky 1985a,b,c; 1986). Most significantly, these simulations have tracked the nonlinear evolution of unstable spherical and axisymmetric clusters, including those with rotation (Abrahams et al. 1994; Shapiro, Teukolsky, & Winicour 1996), and have determined their final fate (see Fig. 1.4). This computational enterprise (“relativistic stellar dynamics on a computer;” see Shapiro & Teukolsky 1992 for a review and references) has demonstrated the following:

- (1) the dynamical collapse of a collisionless cluster leads to the formation of a Kerr black hole whenever  $J/M^2 \lesssim 1$ ;
- (2) collapse leads instead to a bounce followed by virialization of the cluster by relativistic violent relaxation whenever  $J/M^2 \gtrsim 1$ ;
- (3) in extreme core-halo systems, collapse leads to a new stationary, equilibrium system consisting of a central black hole surrounded by an extensive, nearly Newtonian halo containing most of the mass.

Conclusion (3) is very tantalizing as a plausible route for forming SMBHs (see Fig. 1.5 and 1.6). But a key question remains: under what circumstances can a cluster be driven to a dynamically unstable, relativistic state to trigger such a collapse?

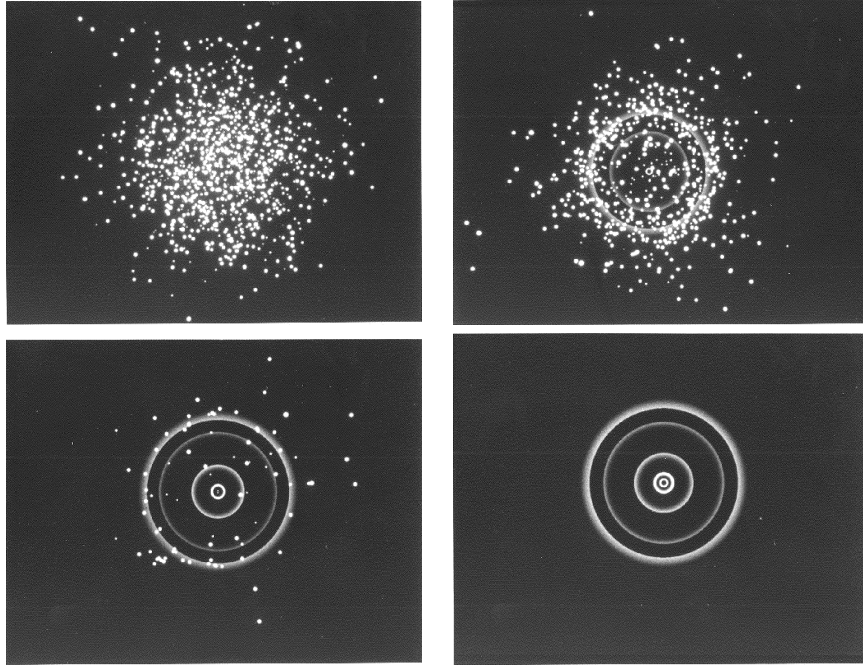


Fig. 1.4. The collapse of a marginally unstable gas of collisionless particles of arbitrary mass  $M$  which at  $t = 0$  obeys a Maxwell-Boltzmann distribution function with an areal radius  $R/M = 9.0$ . Spherical flashes of light are used to probe the spacetime geometry; at late times the light rays are trapped by the gravitational field. Their trajectories help locate the black hole event horizon, which in this example eventually reaches  $r_s/M = 2$  and encompasses all the matter. (After Shapiro & Teukolsky 1988.)

One possibility may involve the “gravothermal catastrophe,” the runaway core contraction on a relaxation timescale of a stable, virialized cluster due to the perturbative influence of collisions (Chandrasekhar 1942; Lynden-Bell & Wood 1968; see Spitzer 1975, 1987 and Lightman & Shapiro 1978 for reviews and references). Collisional scattering is a source of kinetic energy transport (heat conduction). Self-gravitating, nearly collisionless clusters with  $t_d/t_r \ll 1$  have negative heat capacity: as their high-temperature cores lose energy to their low-temperature halos by heat conduction, the cores contract and, in accord with the virial theorem, become hotter still, leading to a thermal runaway. The result is that the clusters undergo homologous core contraction (Lynden-Bell & Eggleton 1980), as depicted in Figure 1.7 for Newtonian clusters composed of identical particles. Contraction to a singular state is complete in a time  $\approx 300t_r(0)$ , where the central relaxation timescale  $t_r(0)$  is measured from an arbitrary initial time  $t = 0$  (Cohn 1979). Specifically, as  $t \rightarrow 300t_r(0)$ , the central density as well as the central redshift, potential and velocity dispersion (temperature) all blow up:  $\rho_c \rightarrow \infty$  and  $z_c \sim \Phi_c \sim v_c^2 \rightarrow \infty$ . At the same time the core radius and mass both shrink:  $r_c \rightarrow 0$  and  $M_c \rightarrow 0$ . The required number of relaxation timescales to reach this singular state, as well as the  $r^{-2.2}$  fall-off in the halo density profile, are nearly independent of the velocity dependence of the collision cross section (Balberg & Shapiro, unpublished).

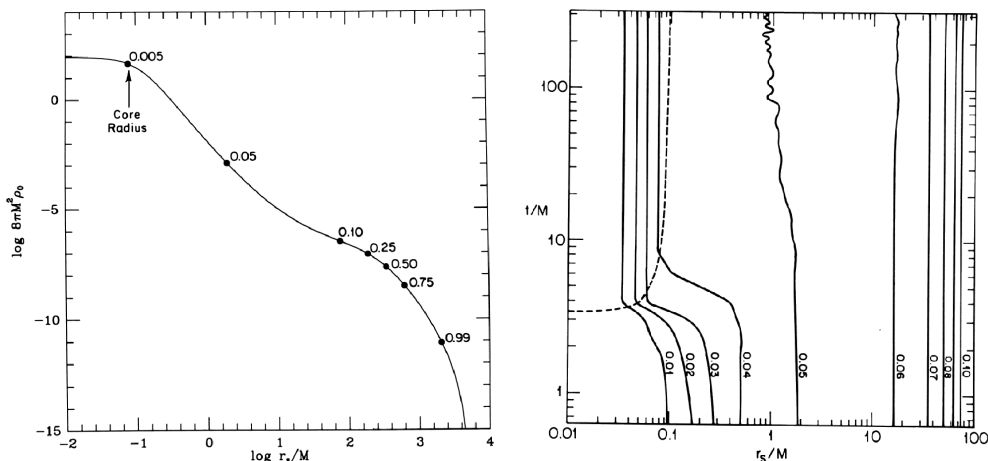


Fig. 1.5. An extreme core-halo configuration of arbitrary mass  $M$  constructed from an  $n = 4$  relativistic polytropic distribution function. The *left* panel shows the initial equilibrium rest-mass density profile. The points label the interior rest-mass fraction. This cluster has a highly relativistic core and an extensive Newtonian halo and is marginally unstable to collapse. The *right* panel is a spacetime diagram showing the worldlines of imaginary Lagrangian matter tracers. The dashed line shows the event horizon of the black hole that forms at the center. Note that the central core and its surroundings undergo collapse but that 95% of the cluster mass settles into stable dynamical equilibrium about the central hole. (From Shapiro & Teukolsky 1986.)

This gravothermal catastrophe can, in principle, drive a core to a highly relativistic state, at which point it could become dynamically unstable to catastrophic collapse on a dynamical timescale.

Detailed numerical calculations have been performed for several scenarios to test whether the gravothermal catastrophe can trigger the formation of SMBHs. We will summarize three of them below.

### 1.5.1 Gravothermal evolution of a cluster of compact stars

Here we describe simulations involving the evolution of clusters of compact stars (neutron stars or stellar-mass black holes) and the build-up of massive black holes. This route has been discussed by several authors (e.g., Zel'dovich & Podurets 1965; Rees 1984; Shapiro & Teukolsky 1985c; Quinlan & Shapiro 1987, 1989). We briefly summarize below the key results of the multi-mass Fokker-Planck calculations of Quinlan & Shapiro (1989).

Consider a dense cluster of compact stars composed initially of identical neutron stars or black holes of mass  $m_* = 1.4 M_\odot$  in virial equilibrium. Take the central mass density to be  $\rho_c \approx 10^8 M_\odot \text{pc}^{-3}$  and the central velocity dispersion to be  $v_c \approx 500 \text{ km s}^{-1}$ . Here gravothermal evolution is driven by the cumulative effect of repeated, distant, small-angle, gravitational (Coulomb) scatterings between the stars. Binary formation is significant and is dominated by dissipative, 2-body capture by gravitational radiation.

The simulations reveal that mass segregation causes significant departures from single-component homological evolution models. For example,  $v_c$  does not increase at the center

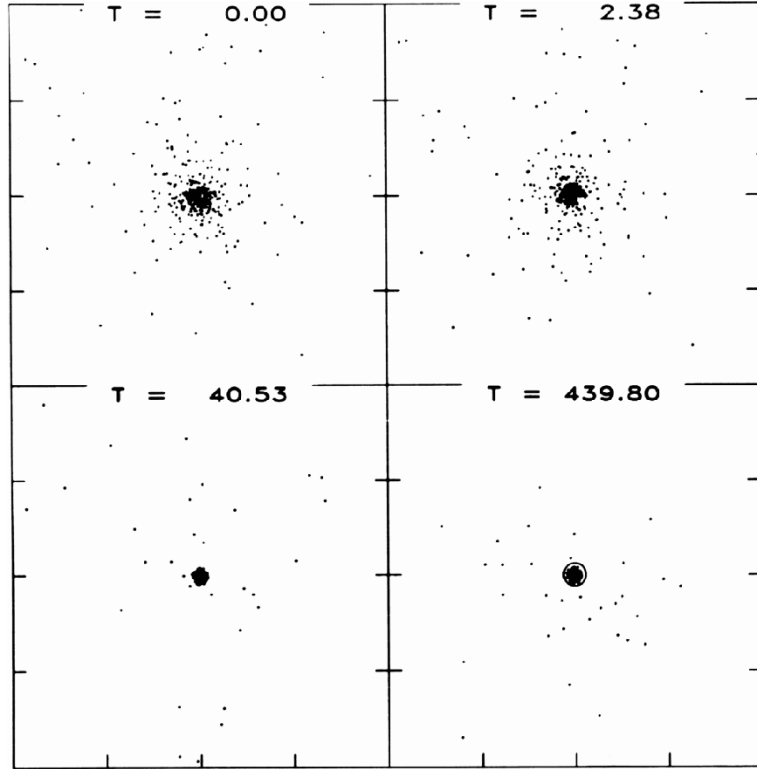


Fig. 1.6. Snapshots of the central particle distribution inside  $r_s/M = 2$  at selected times during the collapse described in Figure 1.5. The cluster does not evolve appreciably after  $t/M = 40$ . The circle in the last frame shows the black hole event horizon at  $r_s/M = 0.1$ . (From Shapiro & Teukolsky 1986.)

and the cluster is not driven to a relativistic state. However, there is an inevitable build-up of massive BHs via successive binary mergers. The evolution is followed up to the formation of BHs of mass  $M_{\text{BH}} \gtrsim 100 M_{\odot}$ , at which point the number of stars in the core become sufficiently small that the Fokker-Planck treatment breaks down. The intermediate mass BH binaries produced in this scenario would be prime sources of gravitational waves for the ground-based network of laser interferometers now under construction (LIGO, VIRGO, GEO, and TAMA) and for the space-based interferometer currently being designed (LISA).

### 1.5.2 Gravo-thermal evolution of a dense cluster of ordinary stars

Here we discuss simulations that start from more typical initial conditions. These calculations treat the gravo-thermal evolution of a dense cluster of ordinary, main-sequence stars (Spitzer & Saslaw 1966; Colgate 1967; Sanders 1970; Begelman & Rees 1978; Lee 1987; Quinlan & Shapiro 1990; Gao et al. 1991; Portegies Zwart & McMillan 2002). Here we briefly summarize the multi-mass Fokker-Planck calculations of Quinlan & Shapiro (1990), which are among the most detailed for galactic nuclei that do not assume the presence of a SMBH *a priori*.

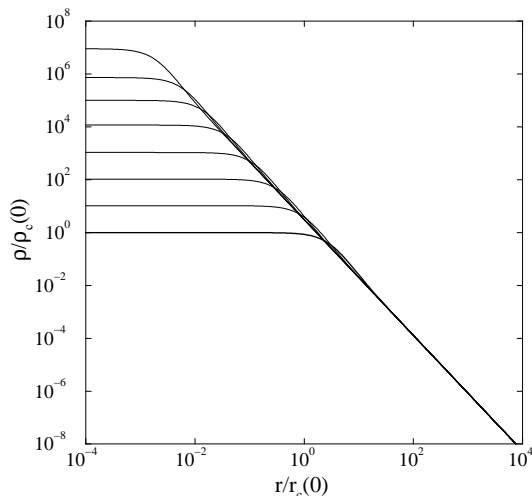


Fig. 1.7. Snapshots of the self-similar density profile at selected times during *secular* core collapse of a nearly collisionless Newtonian cluster (the gravothermal catastrophe). The thick line shows the profile at  $t = 0$  and successive profiles with higher central densities correspond to later times. (From Balberg, Shapiro, & Inagaki 2002.)

Consider a dense galactic nucleus initially consisting of main-sequence stars with mass  $m_* = 1.0 M_\odot$  in virial equilibrium. Take the central mass density to be in the range  $\rho_c \approx 10^6 - 10^8 M_\odot \text{ pc}^{-3}$  and the central velocity dispersion to be in the range  $v_c \approx 100 - 400 \text{ km s}^{-1}$ . This velocity is below the escape velocity from the surface of the stars, so that collisions will lead to mergers and not disruptions. Collisions and mergers, stellar evolution and the formation of new stars from gas liberated by supernovae are included in the calculation, as are the formation of binaries by 3-body encounters and the interaction between hard binaries and single stars. All of this activity takes place in the context of the gravothermal evolution of the cluster, which again is driven by the cumulative effect of repeated, distant, small-angle, gravitational scattering of the stars.

The outcome of the evolution is that stars with  $m_* \gtrsim 100 M_\odot$  form easily, then merge and collapse to form seed BHs with masses  $M_{\text{BH}} \approx 100 - 1000 M_\odot$  in a time  $t \lesssim 10^{10}$  yrs. The end result is the formation of a dense cluster of compact remnants comprised of intermediate mass black holes. The cluster is characterized by frequent binary mergers ( $\gg 1$  per year when integrated throughout the visible universe of  $\sim 10^{10}$  galaxies). These intermediate mass black hole binaries are again promising sources of gravitational waves for the ground-based laser interferometers like LIGO and for the proposed space-based interferometer LISA.

### 1.5.3 Gravothermal contraction of an SIDM halo to a relativistic state

Dark matter comprises about 90% of the matter in the universe. The simplest description of dark matter which accounts for many features of the large-scale structure of the universe is the “cold dark matter” (CDM) model, in which the dark matter particles are essentially collisionless. However, the possibility that dark matter particles interact with

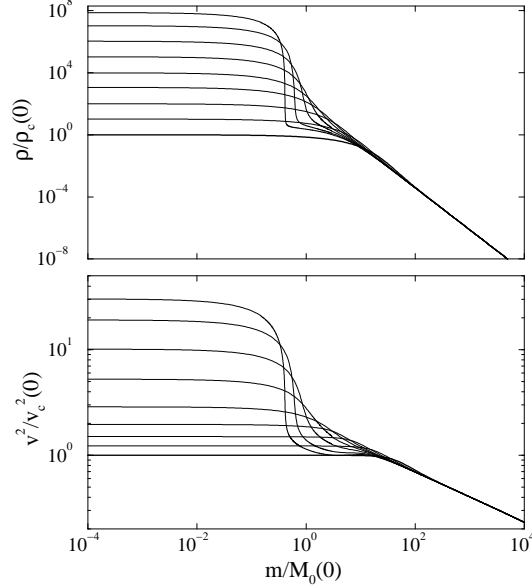


Fig. 1.8. Snapshots of the (a) density and (b) velocity dispersion profiles of an SIDM halo at selected times during gravothermal evolution. The thick line shows the profile at  $t = 0$  and successive profiles with higher central densities correspond to later times. Bifurcation into a fluid inner core and a collisionless outer core is evident at late times. (From Balberg et al. 2002.)

each other strongly and have a substantial scattering cross section has been revived recently (Spergel & Steinhardt 2000) to explain several observations of dark matter structures on the order of  $\lesssim 1$  Mpc. Dynamical studies confirm that halos formed from such “self-interacting” dark matter (SIDM) have flatter density cores in better agreement with the observations than the more cuspy profiles predicted by standard CDM.

Balberg & Shapiro (2002) have recently demonstrated that SMBH formation may be an inevitable consequence of dynamical core collapse following the gravothermal catastrophe in SIDM halos. This conclusion follows from their earlier dynamical study (Balberg et al. 2002) which tracked the gravothermal evolution of a virialized, spherical SIDM halo by employing the fluid formalism of Lynden-Bell & Eggleton (1980). In the early universe, halos form with a Press-Schechter (1974) distribution. Typical halos are characterized by a central mass density  $\rho_c \gtrsim 10^{-2} M_\odot \text{pc}^{-3}$ , a central velocity dispersion  $v_c \gtrsim 100 \text{ km s}^{-1}$  and an elastic scattering cross section  $\sigma \gtrsim 0.1 \text{ cm}^2 \text{ gm}^{-1}$ . The ratio of the scattering mean free path  $\lambda$  to the gravitational scale height  $H$  everywhere satisfies the long mean free path inequality  $\lambda/H \gg 1$  initially. This results in homologous gravothermal contraction at first (see Fig. 1.7). However, in SIDM halos the interactions are large-angle scatterings between close neighbors, not cumulative, small-angle Coulomb scatterings by distant particles, as in star clusters. Consequently, in contrast to star clusters, the inner core of an SIDM halo evolves into the short mean free path (fluid) regime where  $\lambda/H \ll 1$ . There is a bifurcation of the halo into a fluid inner core surrounded by a collisionless outer core and halo (see

*S. L. Shapiro*

Fig. 1.8). Continued heat conduction out of the inner core drives it to a relativistic state, which eventually becomes unstable to collapse to a black hole.

The initial mass of the black hole will be  $10^{-8} - 10^{-6}$  of the total mass of the halo. Very massive SIDM halos form SMBHs with masses  $M_{\text{BH}} \gtrsim 10^6 M_{\odot}$  directly. Smaller halos believed to form by redshift  $z \approx 5$  produce seed black holes of mass  $M_{\text{BH}} \approx 10^2 - 10^3 M_{\odot}$  which can merge and/or accrete to reach the observed SMBH range. Significantly, this scenario for SMBH formation requires no baryons, no prior star formation and no other black hole seed mechanisms (cf. Ostriker 2000; Hennawi & Ostriker 2002).

## 1.6 Conclusions and Final Thoughts

Relativistic gravitation — general relativity — induces a dynamical, radial instability to collapse in *all* forms of self-gravitating matter whenever the matter becomes sufficiently compact. Plausible scenarios have been proposed that can trigger this instability to form SMBHs or their seeds. SMBHs are believed to reside at the centers of quasars, AGNs, and many, if not all, normal galaxies with bulges, including the Milky Way. According to recent observations, even globular clusters may contain black holes of intermediate mass  $\sim 10^3 - 10^4 M_{\odot}$  (Gebhardt, Rich, & Ho 2002; Gerssen et al. 2002), although alternative interpretations have been proposed (Baumgardt et al. 2003). Explaining the origin of SMBHs is thus a fundamental, unresolved issue of modern cosmology and structure formation. Some of the scenarios proposed for forming SMBHs are “hydrodynamical” in nature, as in the collapse of fluid SMSs to SMBHs. Some of them are “stellar dynamical,” as in the collapse of a relativistic cluster of collisionless particles or compact stars. Still others are “hybrids,” as in the case of the collapse of massive stars, built-up by collisions and binary mergers in dense clusters undergoing gravothermal contraction; or the case of the collapse of the fluid inner core of an SIDM halo, following its gravothermal contraction to a relativistic state. The challenge in exploring the competing scenarios is that the different physical regimes characterizing them are described by very different sets of equations, requiring very different numerical techniques for solution. Yet numerical simulations have begun to explore many of the proposed routes.

At the present time we do not know for certain what is the dominant route by which observed SMBHs are formed: Are they born supermassive, or do they grow supermassive from small seeds? Do the seed black holes grow by merger, by gas accretion or both? Do the first black holes arise from the collapse of ordinary baryonic matter, collisionless dark matter, or from some more exotic form of mass-energy (e.g., scalar fields? gravitational waves?).

The growth of black hole seeds by gas accretion is supported by the consistency between the total energy density in QSO light and the BH mass density in local galaxies, adopting a reasonable accretion rest-mass-to-energy conversion efficiency (Soltan 1982; Yu & Tremaine 2002). But quasars have been discovered out to redshift  $z \approx 6$ , so it follows that the first SMBHs must have formed by  $z_{\text{BH}} \gtrsim 6$  or within  $t_{\text{BH}} \lesssim 10^9$  yr after the Big Bang. This timescale provides a tight constraint on SMBH formation. For example, if SMBHs indeed grew by accretion, black hole seeds of mass  $\gtrsim 10^5 M_{\odot}$  must have formed by  $z \approx 9$  to have had sufficient time to reach a mass of  $\sim 10^9 M_{\odot}$  by  $z \approx 6$  (Gnedin 2001).

The correlations  $M_{\text{BH}} \propto L_{\text{bulge}}$  (Kormendy & Richstone 1995) and  $M_{\text{BH}} \propto v_c^4$  (Gebhardt et al. 2000; Ferrarese & Merritt 2000) inferred for galaxies provide important additional constraints. For example, SMBH formation by mergers of smaller seed holes during the

*S. L. Shapiro*

hierarchical build-up of galaxies can account for these scaling laws (Haehnelt & Kauffmann 2000). But some observations suggest that SMBHs spin rapidly. This conclusion might restrict the significance of merger scenarios, since black holes are typically spun down by repeated mergers (Hughes & Blandford 2003). On the other hand, a single final merger with a binary companion of comparable mass could drive the spin of a black hole back up to a large value.

Further observations, including the detection of gravitational waves from distant coalescing black hole binaries, might establish the evolutionary tracts and merging histories of SMBHs and help identify their principle formation mechanism.

This work was supported in part by NSF Grants PHY-0090310 and PHY-0205155 and NASA Grants NAG5-8418 and NAG5-10781 at the University of Illinois at Urbana-Champaign.

## References

- Abel, T., Bryan, G. L., & Norman, M. L. 2000, *ApJ*, 540, 39  
Abrahams, A. M., Cook, G. B., Shapiro, S. L., & Teukolsky, S. A. 1994, *Phys. Rev. D*, 49, 5153  
Balberg, S., & Shapiro, S. L. 2002, *Phys. Rev. Lett.*, 88, 101301  
Balberg, S., Shapiro, S. L., & Inagaki, S. 2002, *ApJ*, 568, 475  
Baumgardt, H., Hut, P., Makino, J., McMillan, S., & Portegies Zwart, S. 2003, *ApJ*, 582, L21  
Baumgarte, T. W., & Shapiro, S. L. 1999, *ApJ*, 526, 941  
———. 2003, *Phys. Reports*, 376/2, 41  
Begelman, M. C., & Rees, M. J. 1978, *MNRAS*, 185, 847  
Bisnovatyi-Kogan, G. S., Zel'dovich, Ya. B., & Novikov, I. D. 1967, *Soviet Astron.*, 11, 419  
Bromm, V., Coppi, P. S., & Larson, R. B. 1999, *ApJ*, 527, L5  
Bromm, V., & Loeb, A. 2003, *ApJ*, in press (astro-ph/0212400)  
Brown, J. D. 2001, in *Astrophysical Sources for Ground-based Gravitational Wave Detectors*, ed. J. M. Centrella (New York: AIP), 234  
Chandrasekhar, S. 1942, *Principles of Stellar Dynamics* (Chicago: Univ. of Chicago Press)  
———. 1964a, *Phys. Rev. Lett.*, 12, 114, 437E  
———. 1964b, *ApJ*, 140, 417  
———. 1969, *Ellipsoidal Figures of Equilibrium* (New Haven: Yale Univ. Press)  
Cohn, H. 1979, *ApJ*, 234, 1036  
Colgate, S. A. 1967, *ApJ*, 150, 163  
Elvis, M., Risaliti, G., & Zamorani, C. 2002, *ApJ*, 565, L75  
Fackerell, E. D. 1970, *ApJ*, 160, 859  
Fan, X., et al. 2000, *AJ*, 120, 1167  
———. 2001, *AJ*, 122, 2833  
Ferrarese, L., & Merritt, D. 2000, *ApJ*, 539, L9  
Fowler, W. A. 1964, *Rev. Mod. Phys.*, 36, 545, 1104E  
Fryer, C. L., Woosley, S. E., & Heger, A. 2001, *ApJ*, 550, 372  
Fuller, G. M., Woosley, S. E., & Weaver, T. A. 1986, *ApJ*, 307  
Gao, B., Goodman, J., Cohn, H., & Murphy, B. 1991, *ApJ*, 370  
Gebhardt, K., et al. 2000, *ApJ*, 539, L13  
Gebhardt, K., Rich, R. M., & Ho, L. C. 2002, *ApJ*, 578, L41  
Genzel, R., Eckart, A., Ott, T., & Eisenhauer, F. 1997, *MNRAS*, 291, 219  
Gerssen, J., van der Marel, R. P., Gebhardt, K., Guhathakurta, P., Peterson, R. C., & Pryor, C. 2002, *AJ*, 124, 3270  
Ghez, A. M., Morris, M., Becklin, E. E., Tanner, A., & Kremenek, T. 2000, *Nature*, 407, 349  
Gnedin, O. Y. 2001, *Class. & Quant. Grav.*, 18, 3983  
Haehnelt, M. G., & Kauffmann, G. 2000, *MNRAS*, 318, L35  
Hennawi, J. F., & Ostriker, J. P. 2002, *ApJ*, 572, 41  
Ho, L. C. 1999, in *Observational Evidence for Black Holes in the Universe*, ed. S. K. Chakrabarti (Dordrecht: Kluwer), 157  
Hughes, S. A., & Blandford, R. D. 2003, preprint (astro-ph/0208484)



*S. L. Shapiro*

- Ipser, J. R. 1969, *ApJ*, 158, 17  
———. 1980, *ApJ*, 238, 1101  
Ipser, J. R., & Thorne, K. S. 1968, *ApJ*, 154, 251  
Kormendy, J., & Richstone, D. 1995, *ARA&A*, 33, 581  
Lai, D., Rasio, F. A., & Shapiro, S. L. 1993, *ApJS*, 88, 205  
Lee, H. M. 1987 *ApJ*, 319, 801  
Lightman, A. P., & Shapiro, S. L. 1978, *Rev. Mod. Phys.*, 50, 437  
Loeb, A., & Rasio, F. A. 1994, *ApJ*, 432, 52  
Lynden-Bell, D., & Eggleton, P. P. 1980, *MNRAS*, 483, 191  
Lynden-Bell, D., & Wood, R. 1968, *MNRAS*, 138, 495  
Macchetto, F. D. 1999, in *Towards a New Millennium in Galaxy Morphology*, ed. D. L. Block et al. (Dordrecht: Kluwer), XX  
New, K. C. B., & Shapiro, S. L. 2001, *ApJ*, 548, 439  
Ostriker, J. P. 2000, *Phys. Rev. Lett.*, 84, 5258  
Portegies Zwart, S. F., & McMillan, S. L. W. 2002, *ApJ*, 576, 899  
Press, W. H., & Schechter, P. L. 1974, *ApJ*, 190, 253  
Quinlan, G. D., & Shapiro, S. L. 1987, *ApJ*, 321, 199  
———. 1989, *ApJ*, 343, 725  
———. 1990, *ApJ*, 356, 483  
Rampp, M., Müller, E., & Ruffert, M. 1998, *A&A*, 332, 969  
Rees, M. J. 1984, *ARA&A*, 22, 471  
———. 1998, in *Black Holes and Relativistic Stars*, ed. R. M. Wald (Chicago: Chicago Univ. Press), 79  
———. 2001, in *Black Holes in Binaries and Galactic Nuclei*, ed. L. Kaper, E. P. J. van den Heuvel, & P. A. Woudt (New York: Springer-Verlag), 351  
Richstone, D., et al. 1998, *Science*, 395, A14  
Saijo, M., Shibata, M., Baumgarte, T. W., & Shapiro, S. L. 2001, *ApJ*, 548, 919  
———. 2002, *ApJ*, 569, 349  
Sanders, R. H. 1970, *ApJ*, 162, 791  
Schödel, R., et al. 2002, *Nature*, 419, 694  
Shapiro, S. L. 2000, *ApJ*, 544, 397  
Shapiro, S. L., & Shibata, M. 2002, *ApJ*, 577, 904  
Shapiro, S. L., & Teukolsky, S. A. 1979, *ApJ*, 234, L177  
———. 1983, *Black Holes, White Dwarfs, and Neutron Stars: The Physics of Compact Objects* (New York: Wiley Interscience)  
———. 1985a, *ApJ*, 298, 34  
———. 1985b, *ApJ*, 298, 58  
———. 1985c, *ApJ*, 292, L41  
———. 1986, *ApJ*, 307, 575  
———. 1988, *Science*, 241, 421  
———. 1992, *Phil. Trans. Roy. Soc. Ser. A.*, A340, 365  
Shapiro, S. L., Teukolsky, S. A., & Winicour J. 1996, *Phys. Rev. D*, 52, 6982  
Shibata, M., Baumgarte, T. W., & Shapiro, S. L. 2000a, *ApJ*, 542, 453  
———. 2000b, *Phys. Rev. D*, 61, 44012  
Shibata, M., & Shapiro, S. L. 2002, *ApJ*, 527, L39  
Soltan, A. 1982, *MNRAS*, 200, 115  
Spergel, D. N., & Steinhardt, P. J. 2000, *Phys. Rev. Lett.*, 84, 3760  
Spitzer, L. 1975, in *IAU Symp. 69, Dynamics of Stellar Systems*, ed. A. Hayli (Dordrecht: Reidel), 3  
———. 1987, *Dynamical Evolution of Globular Clusters* (Princeton: Princeton Univ. Press)  
Spitzer, L., & Saslaw, W. C. 1966, *ApJ*, 143, 400  
Wagoner, R. V. 1969, *ARA&A*, 7, 553  
Wilms, J., Reynolds, C. S., Begelman, M. C., Reeves, J., Molendi, S., Staubert, R., & Kendziorra, E. 2001, *MNRAS*, 328, L27  
Yu, Q., & Tremaine, S., 2002, *MNRAS*, 335, 965  
Zel'dovich, Ya. B., & Novikov, I. D. 1971, *Relativistic Astrophysics, Vol. 1* (Chicago: Univ. of Chicago Press)  
Zel'dovich, Ya. B., & Podurets, M. A. 1965, *Astron. Zh.*, 42, 963 (English translation in *Soviet Astr.-A. J.*, 9, 742)